NRC Research Press

ARTICLE

An empirical method for predicting post-construction settlement of concrete face rockfill dams

Mohammad Kermani, Jean-Marie Konrad, and Marc Smith

Abstract: In this study, employing a database of 19 concrete face rockfill dam (CFRD) cases, two prediction methods for post-construction settlement of CFRDs are presented. In the first method, post-construction settlements are estimated using height of the embankment. In the second method, characterization of the stress–strain behavior of the compacted rockfill layers during construction allows prediction of the subsequent stress–strain–time behavior of the embankment. Knowledge of rock particles strength is necessary in both methods. In the presented methods, settlements are estimated separately for each of the three life-cycle phases: before, during, and after impoundment. The presented results show that, in addition to addressing some limitations of previous methods, the proposed approach is precise and highly practical. It also allows a better understanding of rockfill deformation mechanisms. Apart from using this method for predictive purposes, the presented graphs can be used to distinguish unexpected settlement behavior of a CFRD during its post-construction lifespan.

Key words: concrete face rockfill dam (CFRD), rockfill, time-dependent, post-construction, settlement, prediction.

Résumé : Dans cette étude, à partir d'une base de données de 19 barrages en enrochement avec un masque amont en béton (« CFRD »), deux méthodes de prédiction de tassement post-construction de CFRDs sont présentées. Dans la première méthode, les tassements post-construction sont estimés en fonction de la hauteur du remblai. Dans la deuxième méthode, le comportement contrainte–déformation de l'enrochement des remblais lors de la construction permet de prédire le comportement contrainte–déformation–temps subséquent du barrage. La connaissance de la résistance des particules rocheuses est nécessaire avec les deux méthodes. Pour ces deux méthodes, les tassements en crête sont estimés séparément pour chacune des trois phases du cycle de vie d'un barrage : avant, pendant et après la mise en eau du réservoir. Les résultats présentés montrent qu'en plus de surmonter les difficultés reliées aux méthodes actuelles, les approches proposées sont précises et très pratiques. Elles permettent, également, une meilleure compréhension des mécanismes de déformation de l'enrochement. En plus de servir d'outil prédictif des tassements, les relations présentées peuvent être utilisées afin de détecter un comportement atypique d'un CFRD au cours de sa durée de vie.

Mots-clés : barrage en enrochement avec masque amont en béton (CFRD), enrochement, en fonction du temps, post-construction, tassement, prédiction.

Introduction

The origin of rockfill dams can be traced back to the mining region of California Sierras, in the 1850s. Rockfill dams were of the impervious face type, constructed by dumped rockfill, until earth core dams began to be developed in about 1940. The period from 1850 to 1940 is called the early period by Cooke (1984). The dumped (in 18–60 m lifts) concrete face rockfill dams (CFRDs) performed safely, but the leakage problem became more serious as dams became higher, due to high compressibility of dumped rockfill. During the years 1940 to 1970 (called the transition period by Cooke 1984), earth core rockfill dams became more popular due to higher flexibility of earth materials, and consequently more compatibility with dumped rockfill. Additionally, mostly during the period 1955–1965, a transition developed to the use of sluiced rockfill in thinner layers of 3–3.6 m subsequently compacted by construction truck and dozer traffic. The period after 1970, when compacted and sluiced rockfill was used in construction of rockfill dams of both concrete face and earth core type, is called the modern period (ICOLD 2010). This study addresses the post-construction behavior of CFRDs constructed during the modern period.

CFRDs are widely used because of their cost-effectiveness and the similarity of their constituent materials. Like other types of rockfill embankments, CFRDs are not highly prone to instability. However, attention must be paid to their settlement as excessive displacement may cause cracking of the concrete face, which can result in severe leakage. Some examples of modern CFRDs constructed in the 21st century that suffered severe leakage are Campos Novos and Barra Grande dams in Brazil, and the Mohale dam in Lesotho (Marulanda 2013).

Rockfill consists of rock particles having a large diameter (average size of at least 5 cm and maximum size of up to 2 m) with a variety of particle sizes, shapes, and minerals. As a consequence, full scale experimental study of rockfill material is almost impossible. Scale effects are shown to influence the representativeness of the results of laboratory experiments on rockfill (Marachi et al. 1969; Marsal 1973; Ramon et al. 2008; Alonso et al. 2012). Also, limited laboratory samples are not perfect representations of in situ conditions considering the variety of materials used in

Received 2 April 2016. Accepted 9 November 2016.

M. Kermani and J.-M. Konrad. Department of Civil and Water Engineering, Laval University, Pavillon Adrien-Pouliot, 1065, avenue de la Médecine, Quebec City, QC G1V 0A6, Canada.
M. Smith. Hydro-Quebec, 75 René-Lévesque Blvd. West, Montréal, QC H2Z 1A4, Canada.
Corresponding author: Mohammad Kermani (email: kermani.mhmmd@gmail.com).

Fig. 1. Post-construction crest settlement of Bastyan dam (adapted from Hunter and Fell 2002). α, relative settlement rate in semi-log scale.

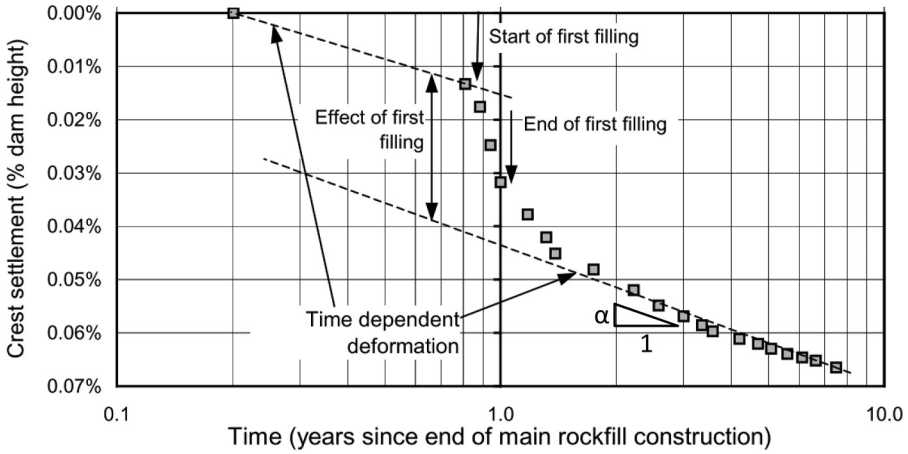

different zones or even in a single zone of a dam. When studying long-term deformations, load application periods are also limited in the laboratory compared to reality. Moreover, no laboratory experiment can apply the same stress path to the sample as in the field.

Numerical models must be calibrated using laboratory experiments, which are prone to the above-mentioned uncertainties. Also, there are uncertainties about using concepts from classical soil mechanics to evaluate the strength and deformation behavior of rockfill. Accordingly, so far, the design of rockfill dams has been mostly based on engineering judgment and experience.

There are several studies in the literature in which settlements of different typical rockfill embankments, including CFRDs, are compared to find a settlement prediction method. These studies are categorized into two groups. The first category consists in studies in which an implicit equation is suggested to calculate dam crest settlement. These equations are mainly of three types: logarithmic strain versus time (Sowers et al. 1965), power type (Soydemir and Kjaernsli 1979), or strain rate versus time (Parkin 1977) relationships.

The second category includes more recent studies, which suggest a qualitative judgment procedure to predict settlements. For instance, Clements (1984), conducting a study on post-construction crest deformations of 68 rockfill dams, suggested predicting the crest settlements by comparing the dam with previously monitored dams with similar characteristics. The major drawback of this approach is that there are many influencing factors that can lead to a high degree of subjectivity. Milligan and Coyne (2005) prepared a database of 95 rockfill dams, with which they questioned the statements of previous researchers who claimed that rockfill dams settle a maximum 0.02% of their height per year after 3 years from the end of construction. They also concluded that because of the considerable amount of variables involved, it is unreliable to use the empirical formulas to predict deformations.

One of the most comprehensive and practical studies on post-construction settlement of CFRDs was carried out by Hunter and Fell (2002). They suggested some empirical methods to predict the rockfill modulus during construction, crest settlement due to impoundment, and the rate of time-dependent crest settlement. They divided the post-construction deformations into two parts: time dependent crest settlements and crest settlement under stresses from first filling. For the post-construction settlements, they suggested that the time datum begin at the end of main rockfill zone construction. The crest settlement attributed to first filling takes place from the beginning of impoundment to a limited time after the end of impoundment. The two components are shown in Fig. 1 for the Bastyan rockfill dam. Hunter and Fell (2002) suggested that the rate of long-term crest settlement, α, as well as the crest settlement attributed to first filling can be estimated considering dam height, the rockfill placement method and the unconfined compressive strength (UCS) of rockfill materials.

In this study, first, the empirical method for prediction of the post-construction settlements of CFRDs by (Hunter and Fell 2002) is modified by changing the time datum for the settlements after impoundment and considering different relative crest settlement rates for the periods before and after impoundment. Also, using a data base of 19 CFRD cases, a novel prediction method is presented using behavior of the embankment during construction. Then, comparing the relative settlement rates before and after impoundment, some aspects of long-term mechanical behavior of compacted rockfill material are put into perspective. Finally, an example application of the prediction methods is presented.

Post-construction crest settlement prediction methods

In the method presented here, it is assumed that the post-construction deformations take place in three phases: (*i*) time-dependent deformations after construction and before impoundment; (*ii*) deformations during impoundment; and (*iii*) time-dependent deformations after impoundment (Fig. 2*a*). The settlements attributed to each phase are calculated separately.

For the time-dependent deformations after construction and before impoundment, the time datum is the end of construction. However, for the long-term crest settlements after impoundment, the time datum is the end of impoundment. This has two major advantages.

First, as the stresses inside the dam body change during the impoundment period and stay almost constant after the end of impoundment, it is reasonable that the time datum for the time-dependent deformations be the end of impoundment. Therefore, the settlement rate values (α_2 in Fig. 2*b*) are more representative values, when comparing to settlement rate, α, values in Fig. 1. This is the same concept as setting the time to zero for every load increment within an oedometer test.

Second, as it is shown in Fig. 2*a* for Bastyan dam and observed in almost all of the case studies, it takes almost 1 year after the impoundment for the settlement data points to fall onto a line in semi-log scale. In the method presented by Hunter and Fell (2002), it is assumed that deformations that take place from the beginning of impoundment to the end of this time lag are attributed to the effect of first filling. Also, no indication was given as to how the length of this delay can be calculated. Because of the nature of graphs drawn by logarithmic scale, this delay changes the crest settlement calculations significantly. Therefore, making settle-

Fig. 2. Post-construction crest settlement of Bastyan dam (*a*) time datum at the end of main rockfill construction; (*b*) time datum at the end of impoundment (data from Hunter and Fell 2002). [Color online.]

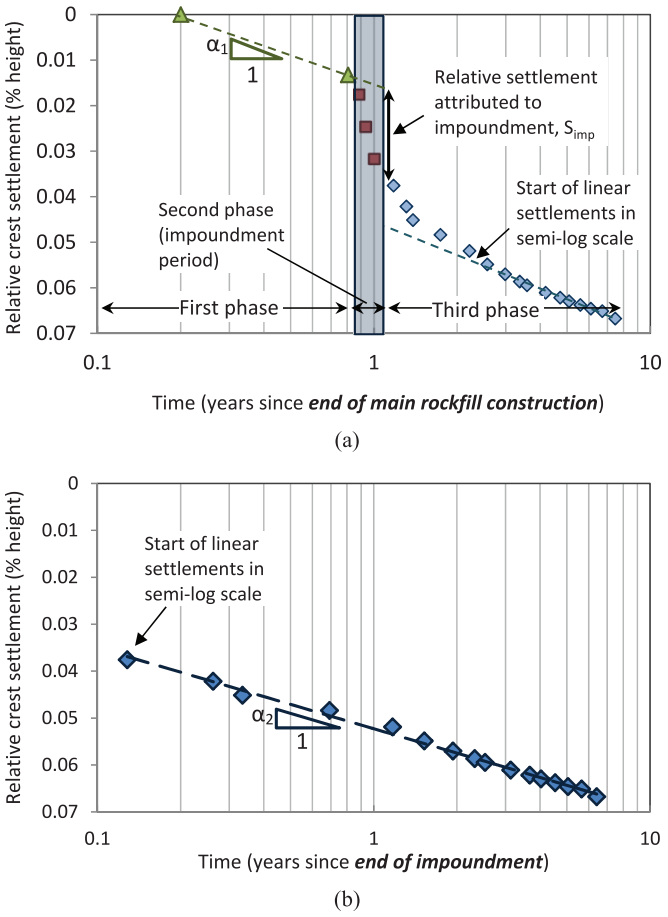

ment predictions using the method presented by Hunter and Fell (2002) is complicated.

On the contrary, in this study, by changing the time datum, the data points after the impoundment will lie on a line in semi-log scale almost right after the end of impoundment (Fig. 2*b*). Therefore, if the time datum is set to the time after which stresses remain almost constant in the embankment, i.e., end of impoundment, the settlement of the crest will fall on a line in a semi-log graph. This is in line with the generally observed behavior of rockfill materials, which show logarithmic creep deformations with time (e.g., Sowers et al. 1965; Marsal 1973; Clements 1981; Alonso et al. 2005). It also allows using this approach to predict the post-construction deformations.

To develop a prediction method, for the two time-dependent phases, the crest settlement rates per height of embankment (relative crest settlement rates, α_1 after main rockfill construction and α_2 after impoundment in Fig. 2*a* and Fig. 2*b*, respectively), and for the reservoir filling phase the maximum crest settlement attributed to impoundment per height of the embankment (relative crest settlement attributed to impoundment, S_{imp} in Fig. 2*a*) are considered. The crest settlements, as well as dam heights, were normally measured at cross-sectional locations with maximum height for each case. For all three phases, the crest settlement is shown to be predictable, knowing UCS of intact rock and one of the following: dam height or the rockfill mechanical behavior during construction. To take strength of rockfill particles into account, the data are presented separately for the dams constructed of high strength rockfill zones, or, of very high strength rockfill zones as classified by the Australian code (Table 1). This means that the rockfill used in the construction of the dam has been extracted from quarries, where the intact rock has been characterized to have the average strength classified as high or very high strength within Table 1.

Table 1. Classification of unconfined compressive strength (UCS) of rock according to Australian code AS 1726–1993 (data from Hunter and Fell 2002).

Strength descriptor	UCS range (MPa)
Extremely high	>240
Very high	70–240
High	20–70
Medium	6–20

In this study, no case with dumped rockfill was studied because of the lack of quality and quantity data in such cases. Therefore, here, the placement method is not directly considered as an influencing factor. Also, as the rockfill used in all of the studied cases is of quarried origin, the influence of shape of particles could not be studied.

The database used in this study is mostly adapted from Hunter and Fell (2002), but also from (Kermani 2016). Nevertheless, the cases with high quality data on post-construction deformations as well as behavior during construction are chosen. Table 2 presents a summary of embankment and rockfill properties for the case studies. The CRFD cases constructed of very high strength rockfill materials (above) are separated with a line from the cases of high strength rockfill (below).

A typical cross section of a modern CFRD is shown in Fig. 3. The main rockfill zones are zones 3B and 3C. Usually, rockfill is coarser and is placed in thicker layers in zone 3C compared to zone 3B (layer thickness and maximum rock diameter are usually limited to 1 m for zone 3B, and 2 m for zone 3C). The central variable zone in this figure shows variations in the size of these two zones in design practice around the world. Zones 1A and 1B are earthfill zones, and zones 2B and 3A support the concrete face slab. The data presented in Table 2 are mostly associated with rockfill placed in zone 3B and also in zone 3C.

Post-construction crest settlement prediction method using dam height and rock strength

In the following, the three phases of post-construction settlement are compared with dam height for different rock strength categories. The adopted concept is the same as Hunter and Fell (2002); however, here, the time datum for the third phase is moved to the end of impoundment and different rates are considered for the relative crest settlements before and after impoundment. Additionally, the crest settlement attributed to first filling is considered to finish by the end of impoundment period. These changes yield more consistent results and facilitate the application of the prediction method.

Crest settlement rate before beginning of impoundment versus dam height

Figure 4 presents relative crest settlement rates after the end of construction and before start of impoundment versus corresponding dam heights. Despite the lack of data for dams of high strength rockfill, the graph shows an increase in the relative crest settlement rate with height. The effect of dam height on the relative crest settlement rates in this phase is associated with the fact that the rate of creep deformation of rockfill material is a function of stress level.

Extrapolating from the trendlines drawn in Fig. 4, the settlement rate is negligible for dams with heights of less than around 25 to 40 m for high strength and very high strength rockfills, respectively. In other words, at stress levels smaller than certain values, rockfill time-dependent deformations are not significant.

Table 2. List of the studied CFRDs (data mostly from Hunter and Fell 2002).

Dam name	Location	Year completed	Max. dam height (m)	Dam crest length (m)	Intact rock strength category	Rockfill source	UCS (MPa)	Dry density (t/m^3)	Rockfill void ratio	Compaction specifications[†]
Bastyan	Tasmania	1983	75	430	EHS to VHS	Rhyolite	—	2.2	0.23	20% W; 1.0 m; 8p; 10 t
Cethana	Tasmania	1971	110	213	VHS	Quartzite	—	2.07	0.27	15% W; 0.9 m; 4p; 10 t
Foz Do Areia	Brazil	1979	160	828	HS to VHS	Basalt, basaltic breccia	185.5[*]	2.12	0.33	25% W; 0.8 m; 4p; 10 t
Murchison	Tasmania	1982	94	200	VHS	Rhyolite	148	2.27	0.23	20% W; 1.0 m; 8p; 10 t
Outardes 2 main dam	Canada	1978	45.7	347.5	VHS	Gneiss, biotite	—	—	—	No W; 1.0 m; 4p; 10 t
Reece	Tasmania	1986	122	374	EHS to VHS	Dolerite	225[*]	2.287	0.29	5%–10% W; 1.0 m; 4p; 10 t
Shuibuya	China	2007	233	675	VHS?	?	—	2.3	0.22	20% W; ?; ?
Toulnustouc south dyke	Canada	2004	46	400	VHS	Gneiss	118	—	—	No W; 0.9 m; 4p; 15 t
Toulnustouc main dam	Canada	2004	76	535	VHS	Gneiss	118	—	—	No W; 0.9 m; 4p; 15 t
Kangaroo Creek	Australia	1969	60	178	MS to HS	Schist	25	2.34	0.20	100% W; 0.9 m; 4p; 10 t
Kotmale	Sri Lanka	1984	90	560	HS to VHS	Charnockitic–gneissic	—	2.2	—	30% W; 1.0 m; 4p; 15 t
Mackintosh	Tasmania	1981	75	465	MS to HS	Greywacke, some slate	45	2.2	0.24	10% W; 1.0 m, 8p; 10 t
Mangrove Creek	Australia	1981	80	380	HS	Siltstone, sandstone	49[*]	2.24	0.18	7.5% W; 0.45 m, 4p; 10 t
Serpentine	Tasmania	1971	38	134	MS to HS	Quartz schist	—	2.1	0.26	? W; 0.6 m; 4p; 9 t
Tianshengqiao I	China	1999	178	1168	HS	Limestone, mudstone	44[*]	2.2	0.21	? W; 1.0 m; 6p; 15 t
White Spur	Tasmania	1989	43	146	HS to VHS?	Tuff	—	2.3	0.21	10%W; 1.0 m; 4p; 10 t?
Winneke	Australia	1978	85	1050	HS	Siltstone	66	2.07	0.30	15% W; 0.9 m; 4–6p; 10 t
Winscar[‡]	England	1974	53	520	HS?	Millstone grit sandstone	—	2.03	0.28	? W; 1.7 m; 4p; 13.5 t
Xingo	Brazil	1993	140	850	HS to VHS?	Granite gneiss	—	2.15	—	15% W; 1.0 m; 4–6p; 10 t

Note: MS, HS, VHS, and EHS denote medium, high, very high, and extremely high strength, respectively.

[*]Average of different zones of rockfill.

[†]Volumetric added water (W); layer thickness; number of passes (p); and weight of roller, respectively.

[‡]Asphaltic concrete face rockfill dam.

This is consistent with the observations in laboratory oedometer and isotropic loading experiments on granular materials that indicate a threshold stress for stresses lower than which, creep strains are negligible (Marsal 1973; Clements 1981; Colliat-Dangus et al. 1988; Oldecop and Alonso 2007).

Crest settlement attributed to impoundment versus dam height

In CFRDs, the deformations during the impoundment period are associated with an increase in stresses inside the dam body due to the reservoir load on the upstream surface. Simple finite element modelling (further explained in the section titled "Comparison between time-dependent deformations before and after impoundment") shows that during impoundment of CFRDs, both mean and deviatoric stresses increase on the upstream side of the dam body. However, mean stress increases more significantly and consequently, the shear stress ratio decreases. Therefore, the settlement of the crest in this phase is considered to occur mostly due to increase in the mean stress.

In addition to the stress level increase, collapse due to wetting might also contribute to the settlements during impoundment. Wetting collapse occurs in rockfill structures due to the strength loss caused by increasing the amount of water in contact with rock particles. The rockfill moisture content might increase due to malfunctions of the concrete face, high downstream water level or penetration of water to downstream rockfill due to excessive precipitations. However, the effect of rockfill wetting collapse is not studied in detail in this paper.

In this study, to obtain the deformations due only to stress increases caused by reservoir loading, the time-dependent component of settlements was subtracted from the total settlements during impoundment. To do so, the rate of time-dependent settlement during impoundment period (second phase in Fig. 2*a*) was assumed to be the same as that in the period before impoundment (first phase in Fig. 2*a*); i.e., α_1.

The relative crest settlements attributed to impoundment values, S_{imp}, are plotted against dam height for the studied CFRDs in Fig. 5. It can be seen that the relative dam crest settlement due to impoundment generally increases with embankment height. The linear trend lines can be used as a guide for a predictive purpose.

The Toulnustouc main dam does not follow the general trend in Fig. 5. Although the relative settlement rates before impoundment (see Fig. 4) and those after impoundment (presented in the next section) are in the expected range, the relative crest settlement due to impoundment is much higher than other similar cases. This unusual behavior can be attributed to the fact that according to Fig. 6, the impoundment of the dam took place mostly in February 2005, but the reservoir reached its maximum level during the snowmelt season, mid-April to mid-June 2005. Although the reservoir level increased much less during the snowmelt season comparing to the previous months (20 versus 50 m), the crest settled much more during this period. The reason might be that because the main rockfill zone of the dam was compacted without watering, the effects of snowmelt along with the subsequent precipitations increased the wetting collapse in the downstream rockfill zones during the impoundment period.

Crest settlement rates after impoundment versus dam height

Relative crest settlement rates after impoundment, α_2, are drawn versus the embankment heights in Fig. 7. For the dams of very high strength rockfill zones, the relative crest settlement rate increases slightly with dam height and is almost similar for all of the cases. The value is less than 0.05 for all of the studied dams. This means that for a 100 m high dam, the crest settlement attributed to time-dependent deformations after impoundment is less than 14 cm in 50 years of operation.

In the CFRDs constructed of high strength rockfill, there is a clear tendency of increasing relative long-term crest settlement rates with dam height. Although Fig. 7 generally correlates with

Fig. 3. Typical zoning of concrete face rockfill dams (adapted from ICOLD 2010).

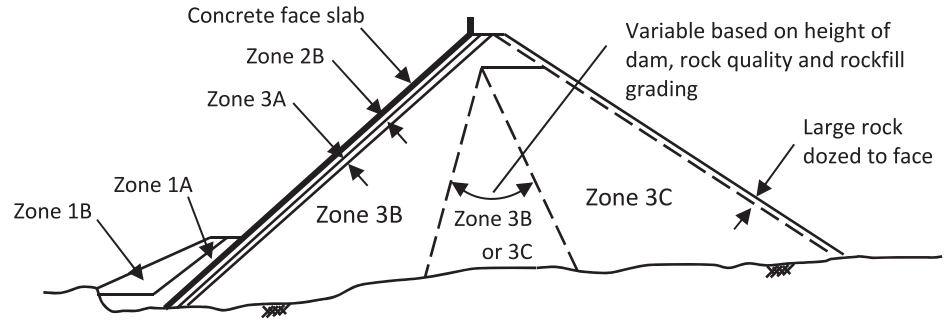

Fig. 4. Relative crest settlement rate before impoundment versus dam height. [Color online.]

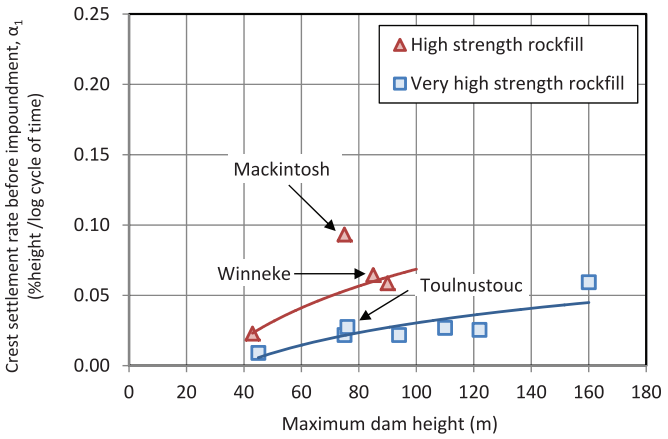

the findings of Hunter and Fell (2002), when comparing the data with an adjusted time datum with the same data presented by Hunter and Fell (2002), more consistent values are obtainable for Kotmale and Winneke dams. Yet, for Winneke, the impoundment began 1.6 years after end of rockfill construction and took 3.8 years to end. Consequently, a large amount of time-dependent deformation had already taken place before and during the impoundment. Therefore, the rate of settlements relative to dam height is lower than expected for this dam. Additionally, because at the Mangrove Creek dam, the impoundment was still ongoing at the end of studied period, i.e., 15 years after end of construction, this dam does not yield any data point in this figure.

Similar to the data presented for post-construction settlements before impoundment, the dependence of relative settlement rates after impoundment on embankment heights tends to decrease with dam height. In other words, the evolution of relative settlement rates with dam height is nonlinear. It is also worth noting that Shuibuya and Winscar dams fall off the general trend in this figure.

Despite the similarity of the general trend of relative settlement rate versus dam height curves before and after impoundment, the relative settlement rate values before impoundment are generally smaller compared to those after impoundment. This aspect will be further examined in this paper.

Post-construction crest settlement prediction method using rockfill modulus and rock strength

The previously presented method has the following limitations:

- The embankment height does not perfectly represent the dam's geometry. Embankment slopes and valley shape are also influencing factors.
- The UCS of intact rock is not the only material parameter that affects the post-construction settlement of CFRDs. To reach a more reliable prediction method, a parameter shall be defined that also takes into account the shape and gradation of particles and the compaction method.

Therefore, a novel approach is introduced here, in which the post-construction settlements are determined using the dam's deformation behavior during construction. This method is adapted from the well-known concept that the secondary compression index C_α and compression index C_c are related for different types of earth materials. In other words, the time-dependent mechanical behavior of a material in constant stress can be estimated through its behavior during loading. The material can be a fine-grained soil (Mesri and Godlewski 1977), sand (Mesri and Vardhanabhuti 2009) or rockfill (Oldecop and Alonso 2007; Cormier and Konrad 2015). In the case of rockfill dams, secondary compression index corresponds to post-construction settlement behavior and compression index corresponds to the rockfill construction period.

In this study, the secant modulus of the main rockfill zone at the end of construction (eq. (1) and Fig. 8) is used to illustrate the behavior during construction. The rockfill secant modulus, for a certain rockfill layer, at end of construction can be defined by dividing the calculated vertical stresses by the strains inferred from readings of settlement gauges

$$E_{RC} = \frac{\sigma_z}{\delta_s/d_1} \quad (1)$$

where σ_z is the stress at the mid-height of the layer, as shown in Fig. 8; δ_s is the vertical displacement of the considered layer; and d_1 is thickness of the considered layer. To calculate the moduli, the stress at the mid-height of the layer σ_z is considered in this paper and is calculated using a simple linear elastic numerical analysis. In this way, the effect of embankment shape on vertical stress is taken into account. Other than Shuibuya, Tianshengqiao, and Winscar dams for which the moduli are calculated by the authors, in this section, the values of modulus during construction, E_{RC}, are taken from Hunter and Fell (2002). These values are calculated for the lower half to one third of the dam height. Note that, this modulus calculation method differs from that of Fitzpatrick et al. (1985), Pinto and Marques Filho (1998), and Giudici et al. (2000), in the sense that first, here, the shape of embankment is considered; i.e., the vertical stress is not simply taken as the multiplication of fill height to fill density. Secondly, to determine the modulus, the vertical stress is calculated in this paper for the mid-height, instead of the top, of the layer. The calculated stress at mid-height is supposed to yield the average vertical stress of the layer. An example of modulus calculation is presented further in this paper.

Crest settlement rate before beginning of impoundment versus rockfill secant modulus

The relative crest settlement rates before impoundment are shown versus rockfill secant modulus at end of construction in Fig. 9. For the dams where the main rockfill zone is constructed of very high strength rockfill, there is a slight decrease in the relative

Fig. 5. Crest settlement per dam height attributed to impoundment versus dam height for studied CFRDs. [Color online.]

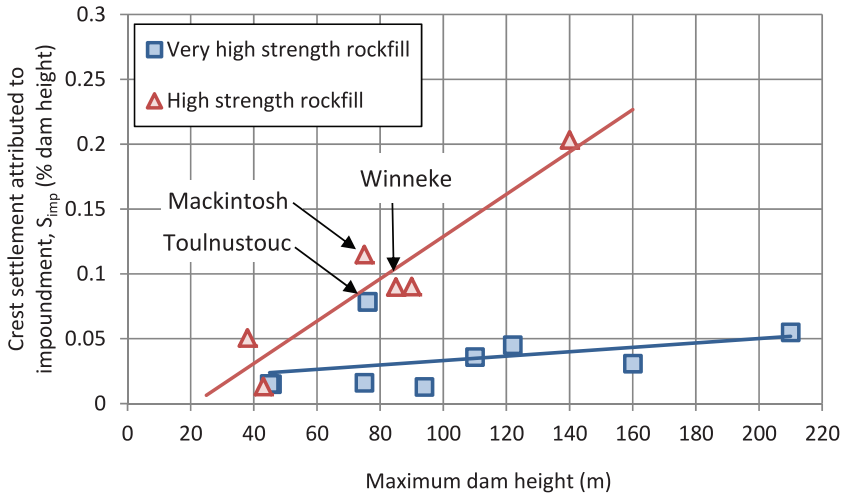

Fig. 6. Evolution of crest settlement per dam height and reservoir water level history of Toulnustouc main dam in the highest section. [Color online.]

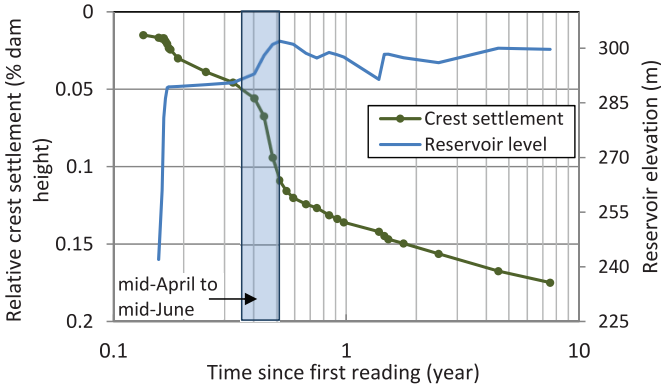

crest settlement rate, α_1, with secant modulus at the end of construction. For the dams where the main rockfill zone is constructed of high strength rockfill, the relative crest settlement rate decreases more clearly with rockfill secant modulus. In other words, the stiffer the rockfill layers are during construction, the less settlement they undergo in the post-construction period. A power law curve is fitted to the curve to allow its use for predictive purposes.

The Mackintosh dam, which was considered as an outlier in Fig. 4 falls inside the generally expected trend in Fig. 9. This shows the reliability of this predictive approach. As the in situ behavior of the same structure is being used for prediction, it reduces the shortcomings of the other prediction approaches.

Crest settlement attributed to impoundment versus rockfill secant modulus

The concept of linking the load–deformation behavior of the dam during construction to its behavior afterwards is also used here. Figure 10 presents the relative crest settlement attributed to impoundment versus average rockfill secant modulus at the end of construction for different CFRDs. Once again, the higher the secant modulus of the rockfill at the end of construction, the lower the dam's relative settlement attributed to impoundment. However, the effect of intact rock strength is not significant here. Except for one case, CFRDs constructed of both very high and high strength rockfill zones lie along the same general trend line. In other words, by comparing the settlements caused by impoundment with rockfill secant modulus, the effect of rock intact strength decreases. Note that, because in the case of CFRDs deformations during both construction and impoundment represent stress–strain behavior of their materials due to gradual increases in stress level, the existence of a relationship between the two phases is quite rational.

Crest settlement rate after impoundment versus rockfill secant modulus

Figure 11 shows the long-term relative crest settlement versus rockfill secant modulus for the studied CFRDs. The same trend as settlement rates before impoundment (Fig. 9) is observed here. The only difference is that, after impoundment, the relative settlement rates are generally higher than those in Fig. 9 and the difference between the trend lines, for the two strength categories, is more evident.

It is interesting to note that despite very high strength of rockfill in Foz Do Areia and Reece dams, the rockfill has low secant modulus at the end of construction, even less than some of the high strength rockfills. Additionally, as can be seen in Table 2, rockfill void ratio is high for the two cases. Therefore, it can be inferred that the void ratio affects the rockfill stress–strain behavior during construction more than the intact strength of rock particles. However, for the time-dependent deformations, the intact strength is more influential.

Winscar and Shuibuya dams, which were outside the trends observed in the graphs of α_2 versus dam height, fall well inside the trend in Fig. 11. This shows the efficiency of the current method. It is also worth noting that the Winneke dam, which was outside the trend observed for the long-term relative crest settlement (after impoundment) of dams constructed of high strength rockfill, is well inside the expected trend in the other two sections (time-dependent settlements before impoundment and settlements attributed to impoundment). This validates the hypothesis that its unexpected behavior during the long-term settlement phase is due to the delay in completion of impoundment.

A summary of the parameters calculated for the studied cases and used in the previous three sections is presented in Table 3.

Comparison between time-dependent deformations before and after impoundment

In this section, the relative crest settlement rates before and after impoundment are compared to study the effect of changes in stress distribution and properties of materials on time-dependent deformation of CFRDs. To compare the stress state inside an embankment before and after impoundment, a generic 100 m high embankment having slopes of 1 vertical to 1.4 horizontal was

Fig. 7. Relative crest settlement rate after impoundment versus dam height. [Color online.]

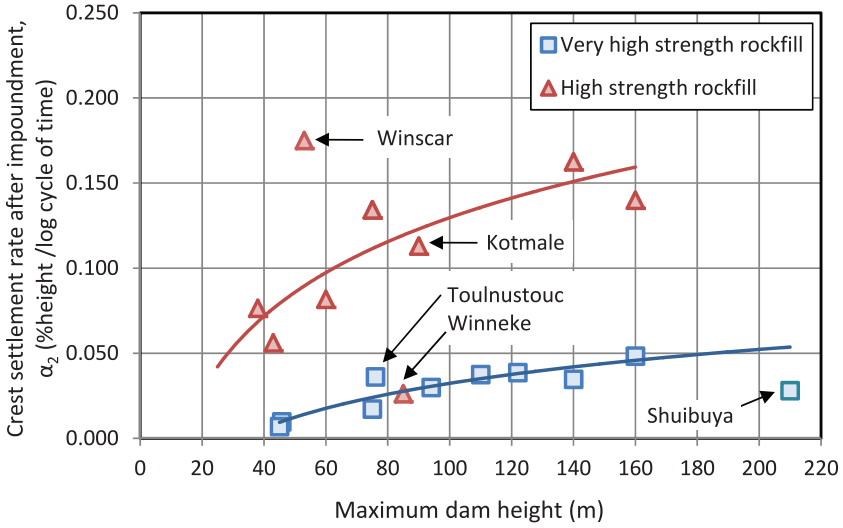

Fig. 8. Calculation of modulus during construction (adapted from Hunter and Fell 2002).

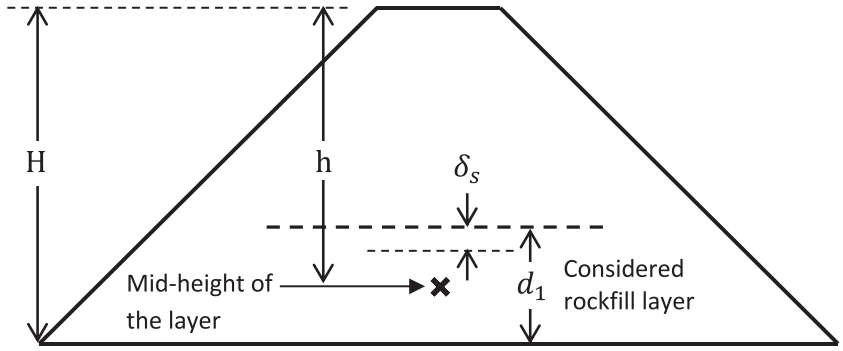

Fig. 9. Relative crest settlement rate before impoundment versus rockfill secant modulus at end of construction. [Color online.]

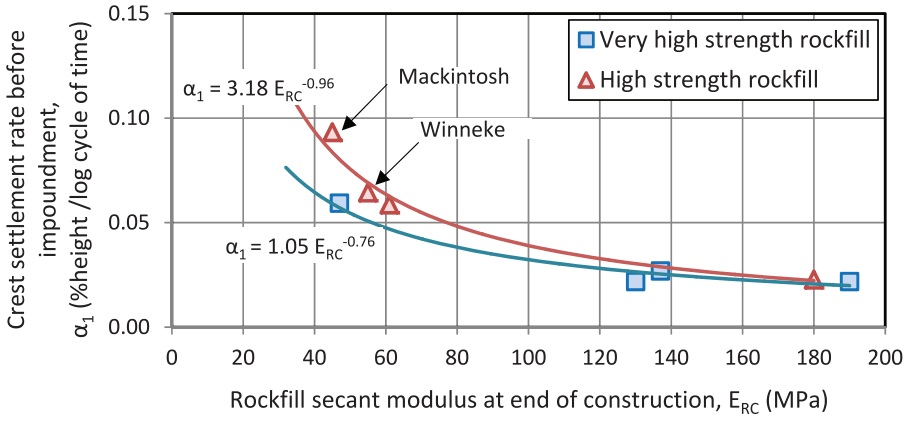

modeled using the Plaxis 2D Hardening soil model. This model, which uses theory of plasticity to reproduce hyperbolic axial strain – deviatoric stress in a drained triaxial test, and, includes soil dilatancy, is quite common in modeling rockfill embankments. The mechanical parameters used for the model are presented in Table 4. In the table, E_{50}^{ref} and E_{ur}^{ref} are the secant modulus in 50% of maximum shear stress and unloading–reloading stiffness in a standard triaxial test, respectively; E_{oed}^{ref} is the tangent stiffness for primary oedometer loading at a reference stress, p^{ref}; and m is the power for stress-level dependency of the stiffness moduli:

$$E \approx E^{ref}(\sigma/p^{ref})^m \quad (2)$$

where E^{ref} is the stiffness at a reference stress, σ is "minimum principal stress" for E_{50}^{ref} and E_{ur}^{ref} and "minimum principal stress over K_0^{nc}" for E_{oed}^{ref}. K_0^{nc} is the K_0 value for normal consolidation, ν_{ur} is Poisson's ratio for unloading–reloading, and R_f is the failure ratio (ultimate over asymptotic deviatoric stress). c, φ, and ψ are cohesion, friction angle, and dilation angle, respectively.

The construction of the generic embankment was modeled using the software's staged construction option in which 10 m lifts

Fig. 10. Relative crest settlement attributed to impoundment versus rockfill secant modulus at end of construction. [Color online.]

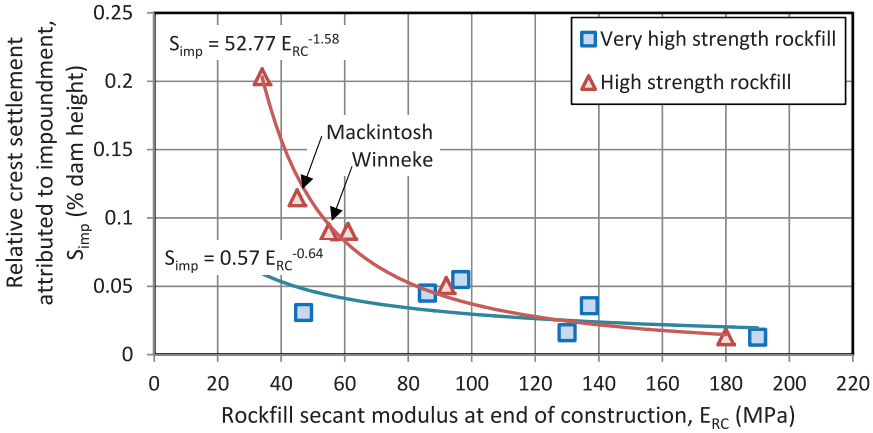

Fig. 11. Relative crest settlement rate after impoundment versus rockfill secant modulus at end of construction. [Color online.]

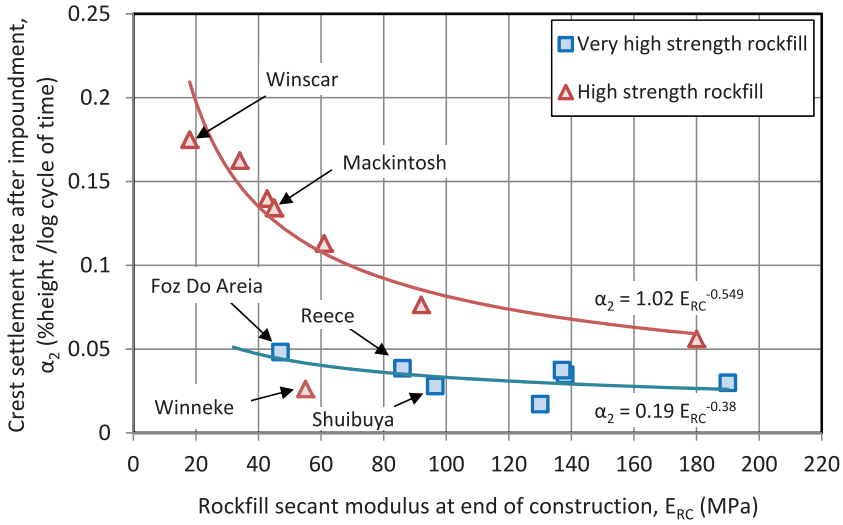

Table 3. Calculated parameters for the studied CFRDs.

Dam name	E_{RC} (Mpa)	α_1 (% height per log time cycle)	S_{imp} (% dam height)	α_2 (% height per log time cycle)	Time from EoC to EoI (years)
Bastyan	130	0.022	0.016	0.017	1.05
Cethana	137	0.027	0.036	0.038	0.48
Foz Do Areia	47	0.059	0.031	0.048	0.90
Murchison	190	0.022	0.013	0.030	1.09
Outardes 2 main dam	—	—	0.015	0.017	0.15
Reece	86	0.026	0.045	0.039	1.46
Shuibuya	96.5	—	0.055	0.028	1.07
Toulnustouc south dyke	—	0.009	0.015	0.007	1.66
Toulnustouc main dam	—	0.028	0.079	0.037	0.53
Kangaroo Creek	—	—	—	0.082	—
Kotmale	61	0.059	0.090	0.113	1.04
Mackintosh	45	0.093	0.115	0.134	2.90
Mangrove Creek	55	—	—	0.285	—
Serpentine	92	—	0.051	0.076	2.90
Tianshengqiao I	43	—	—	0.140	—
White Spur	180	0.023	0.013	0.056	0.24
Winneke	55	0.064	0.084	0.026	5.40
Winscar	17	—	—	0.175	—
Xingo	34	—	0.203	0.163	1.46

Note: EoC, end of construction; EoI, end of impoundment.

Table 4. Hardening soil model parameters used for modeling a generic embankment.

γ (kN/m^3)	E_{50}^{ref} (MPa)	E_{oed}^{ref} (MPa)	E_{ur}^{ref} (MPa)	ν_{ur}	p^{ref} (kPa)	R_f	m	c (kPa)	φ (°)	ψ (°)	K_0^{nc}
23	100	100	300	0.2	100.0	0.9	0.5	0.0	45	10	0.5

Fig. 12. Stress state inside a generic CFRD (*a*) before and (*b*) after impoundment. [Color online.]

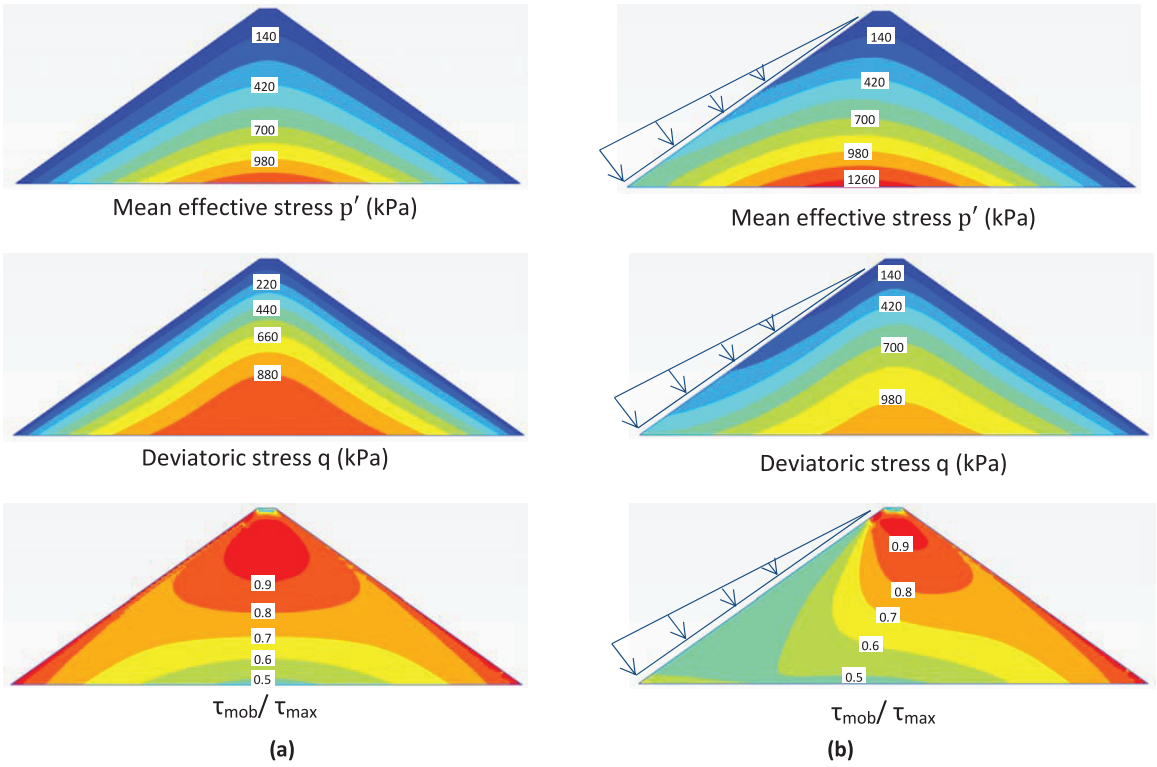

Fig. 13. Relative crest settlement rates before impoundment, α_1, versus after impoundment, α_2. [Color online.]

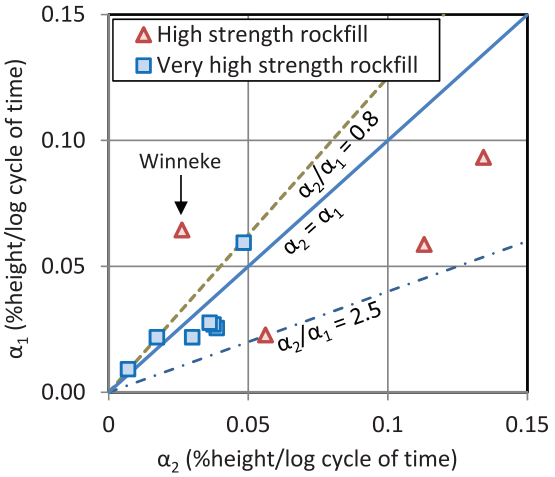

Fig. 14. The ratio of relative crest settlement rates after and before impoundment versus time elapsed from the end of rockfill construction, EoC, to the end of impoundment, EoI. [Color online.]

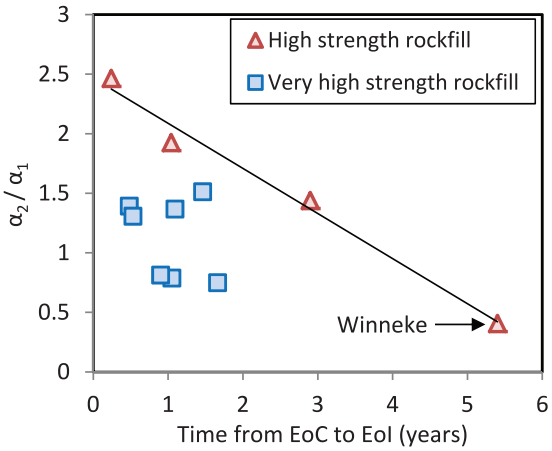

were considered. After construction modelling, the reservoir load was applied on the impervious upstream face in a single stage. The computed mean effective stress, deviatoric stress, and relative shear stress, τ_{mob}/τ_{max}, before and after application of reservoir load are shown in Fig. 12. τ_{mob} is the mobilized shear strength or the radius of the Mohr circle and τ_{max} is the maximum value of the shear stress, for the case when the Mohr circle expands and touches the Coulomb failure envelope considering a fixed center. Therefore, τ_{mob}/τ_{max} is an indicator of the proximity of an element to the failure envelope and varies between 0 for isotropic stress state and 1 for failure state. As can be seen, by applying reservoir load, both mean and deviatoric stresses increase on the upstream side and centerline of the embankment. However, the mean stress increases more significantly and the relative shear stress decreases in the upstream side of the embankment. While stresses generally increase inside the embankment, if considering a Coulomb failure criterion, the material moves away from failure state due to the induced stresses. This is an advantage of CFRDs com-

Fig. 15. Typical cross section of La Yesca dam (adapted from Marengo-Mogollón and Rivera-Constantino 2012).

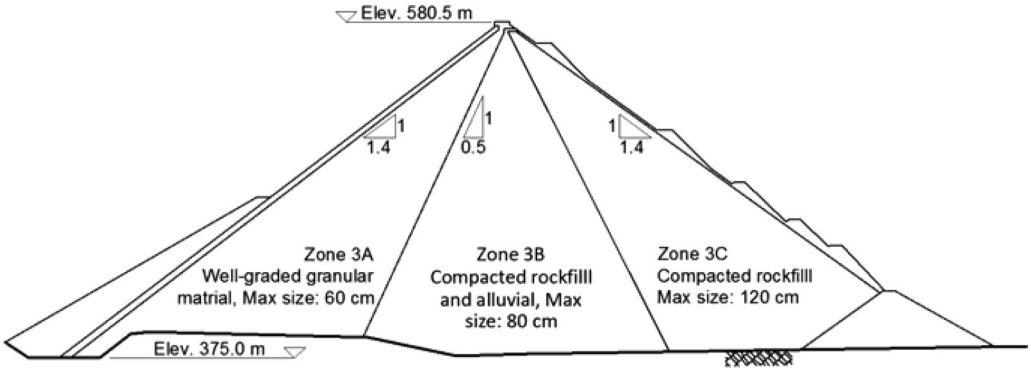

Fig. 16. Contours of settlements (cm) at La Yesca Dam for the end of construction (modified from Marengo-mogollón and Rivera-Constantino 2012). [Color online.]

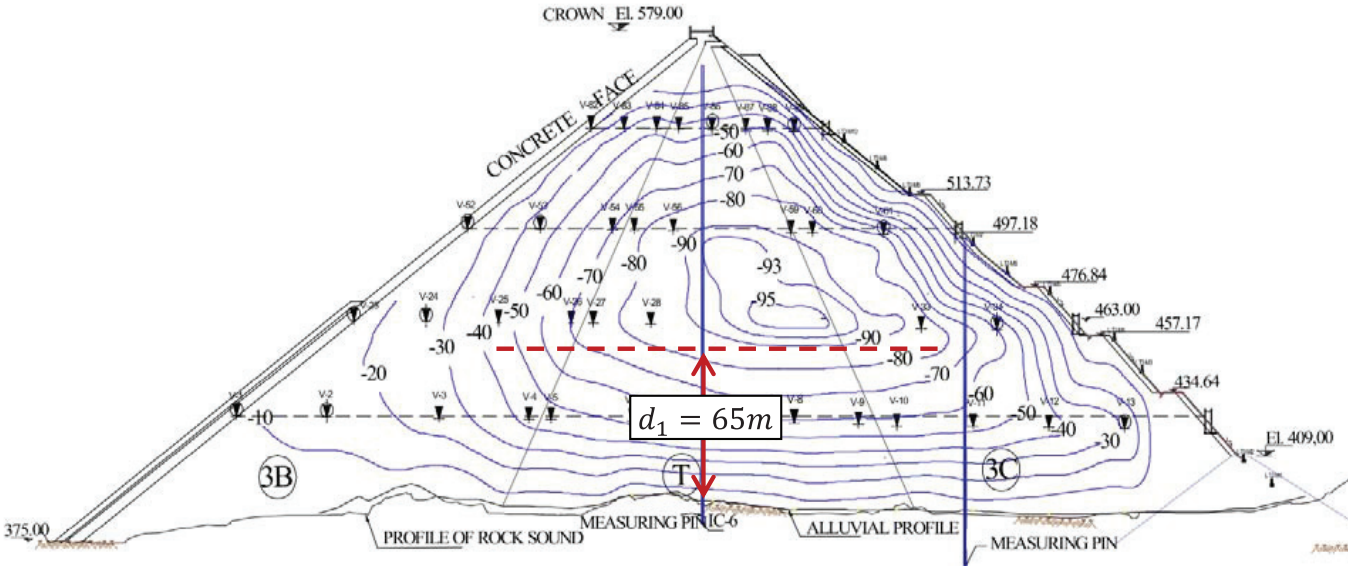

pared to other types of embankment dams, where impoundment increases the risk of slope instability. Additionally, it can be implied that the instantaneous as well as long-term deformations caused by impoundment in a CFRD are mostly due to increase in confining pressure rather than shear stress.

Returning to the data from studied CFRDs, Fig. 13 shows how the settlement rates before and after impoundment compare for different cases. Despite some exceptions, the relative settlement rates become larger after impoundment. Generally, the α_2/α_1 ratio lies between 0.8 and 2.5. The relative crest settlement rate after impoundment, α_2, is very small for Winneke dam because it has undergone a very long settlement period before the end of impoundment (5.4 years). Neglecting this case, generally, the dams constructed of high strength rockfill zones show higher α_2/α_1 values in comparison with those constructed of very high strength rockfill. It can be inferred that for the rockfill of lower strength, the strain rate is more influenced by the stress level than the rockfill of higher strength. This is in accordance with the results of the previous sections where the relative crest settlement rates of dams constructed of very high strength rockfill zones show less dependency on the dam height.

Reservoir impoundment has two influences on the behavior of CFRDs: first, as discussed previously, the stress distribution inside the dam changes due to the load application on the upstream face; second, the rockfill material undergoes changes, some of the cracks inside the particles propagate, and particles break and fill the voids. Additionally, some of the asperities of the particles break. The change in properties throughout time, and normally stiffening of the material, is called the aging effect. The first aspect results in larger time-dependent deformations while the second generally leads to smaller deformations. As can be seen in Fig. 13, in most of the studied cases, the first mechanism prevails (right side of $\alpha_2 = \alpha_1$ line) and in some, the second one is dominant (left side of $\alpha_2 = \alpha_1$ line).

To study aging effect, the ratios of relative crest settlement rates, after and before impoundment, α_2/α_1, are drawn versus the elapsed time between end of construction and end of impoundment (start of the third phase) (Fig. 14). A clear trend can be seen in this figure for the dams constructed of high strength rockfill. As the time interval increases, the ratios of settlement rates decrease. In other words, the longer the time before start of the third phase (the end of impoundment), the more significant the effect of aging and the less the dam's crest settlement in the period afterwards. The Winneke dam, which was considered an outlier in Fig. 13, falls very well inside the trend in Fig. 14. For the dams constructed of very high strength rockfill, in contrast, no clear trend is observed. This may indicate that the aging effect is more influential in the less stiff rockfill, where the particles break more frequently and the voids fill more often between the rock particles. Therefore, the number of interparticle contact points increases and less breakage takes place in the subsequent phase.

Fig. 17. Contours of vertical stress for a generic embankment with 1 horizontal to 1.4 vertical slope at end of construction. *H*, dam height in the section; γ, fill density. [Color online.]

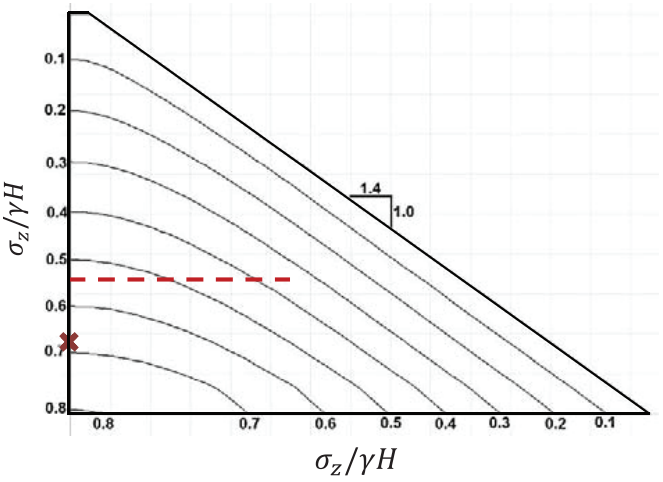

Example of post-construction crest settlement prediction

The La Yesca dam in Mexico, a 208 m high and 628 m long structure, was chosen to permit an actual prediction of the post-construction settlement of a CFRD. This can be considered as a "class B" prediction according to (Lambe 1973) because the results are not known at the time prediction is made. Construction of the dam body began in 2008 and ended in April 2012. As can be implied from the existing data, the impoundment started right after end of construction and ended in September 2013. However, no data on post-construction settlements of the dam were found. The material properties and deformation of the dam during construction are presented in Marengo-Mogollón and Rivera-Constantino (2012). The typical cross section of the dam includes three major zones (Fig. 15). The main embankment zones (3A and 3B) are comprised of rockfill and coarse-grained alluvial soil. Therefore, the La Yesca dam is different from the studied cases in this respect. Despite the lack of detailed data, the UCS of the rockfill (that is originated from ignimbrites) is assumed to be in the very high strength category.

Using dam height and rockfill strength

The height of the maximum section of the dam is 195 m at the centerline from the crest to the foundation. Therefore, using Fig. 4, relative crest settlement rate after construction, α_1, extrapolates 0.055% per log cycle of time. Although the impoundment of the dam started right after end of construction and the first phase does not exist in this case, α_1 must be used to calculate the time-dependent deformations during impoundment. So, considering that impoundment finishes 1 year and 4 months (1.33 years) after end of construction, settlement of

$$S(\%\text{ dam height}) = 0.055 \times \log(1.33/0.1) = 0.06\% \quad \text{or} \quad 12\text{ cm} \tag{3}$$

must be summed with the settlements attributed to first filling to estimate total settlement during impoundment period. The crest settlement attributed to stress increase caused by impoundment can be calculated extrapolating from Fig. 5. Considering the *x* value (dam height = 195 m), the S_{imp} amount is estimated as 0.05% of dam height or 10 cm. Likewise, extrapolating from Fig. 7 (*x* value = dam height = 195 m), the relative crest settlement rate after impoundment is estimated as 0.05% per log cycle of time. Therefore, for instance, in 50 years of operation after impoundment, the relative crest settlement would be 0.052 × log(50/0.1) = 0.14% dam height or 27.5 cm. Note that the beginning of the time interval for

Fig. 18. Post-construction crest settlement prediction of La Yesca dam (*a*) before and (*b*) after the end of impoundment. [Color online.]

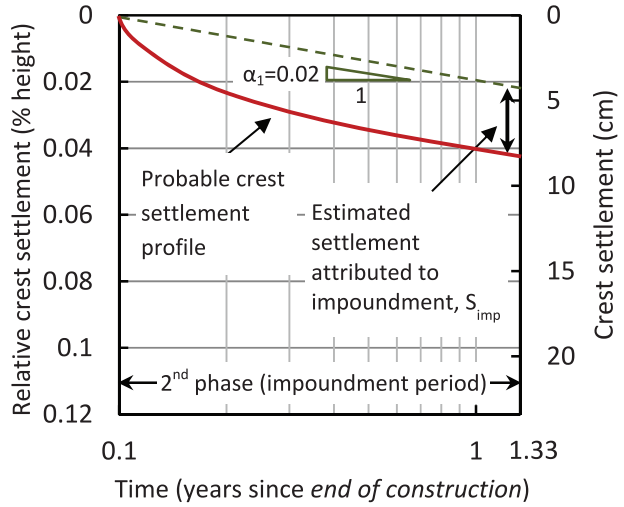

(a)

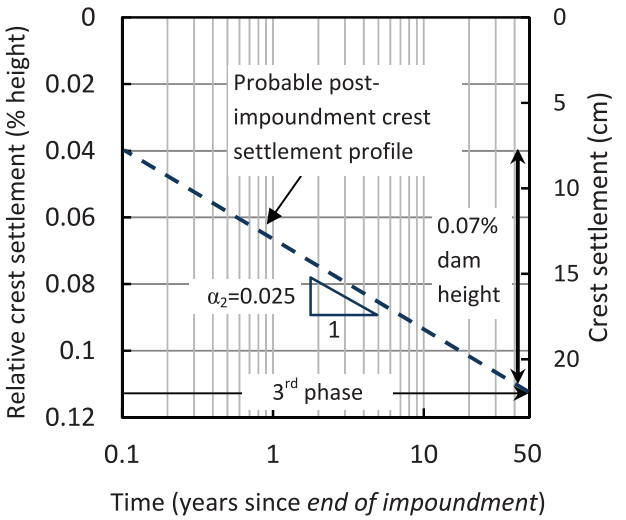

(b)

estimation of settlements in each phase, t_1, is considered to be 0.1 years in the calculations (e.g., in eq. (3)) because it yields acceptable results for the studied cases. Considering smaller values of beginning of the time interval tends to overestimate the settlements.

Using rockfill secant modulus and strength

The vertical deformation contours of La Yesca dam measured with hydraulic levels at end of construction are shown in Fig. 16. As it is indicated, for a layer located in the bottom one third of the dam, the vertical settlement, δ_s, is approximately 80 cm and the layer thickness, d_1, equals 65 m. The vertical stress contours relative to dam height, computed from linear elastic analysis of a generic homogeneous, symmetrical embankment with the same embankment slopes as La Yesca dam, are presented in Fig. 17. Using this figure, the vertical stress at the mid-height of the considered layer (supposedly, the average vertical stress of the layer) can be calculated as

Table 5. Summary of predicted parameters for La Yesca dam.

Parameter used for prediction	α_1 (% per log cycle of time)	Time-dependent settlement during impoundment (cm)	Settlement attributed to impoundment		Settlement after impoundment	
			S_{imp} (% dam height)	(cm)	α_2 (% per log cycle of time)	(cm in 50 years)
Dam height	0.055	12	0.05	10	0.052	27.5
Rockfill modulus	0.02	4.5	0.02	4	0.025	13.5

$$(4a) \quad \frac{\sigma_z}{\gamma H} = 0.68 \Rightarrow \sigma_z = 0.68 \times 20.1 \times 195 = 2665 \text{ kN/m}^2$$

where γ is the unit weight of the overlaying fill layers and H is dam height. Thus, the modulus will be

$$(4b) \quad E_{RC} = \frac{\sigma_z}{(\delta_s/d_1)} = \frac{2861}{(0.8/65)} = 216\,550 \text{ kN/m}^2$$

Conducting the same procedure for two other layers adjacent to the foundation with different thicknesses, an average modulus of 210 MPa was calculated for prediction.

Now, using the calculated rockfill secant modulus, extrapolating from Fig. 9, α_1, equals 0.02% per log cycle of time (time-dependent settlement during impoundment period would equal 0.02% of dam height using the same method as in eq. (3)). Likewise, implementing Fig. 10, the crest settlement attributed to first filling equals 0.02% of dam height, i.e., 4 cm. Also, using Fig. 11, the relative crest settlement rate after impoundment, α_2, equals 0.025% per log cycle of time i.e., 0.07% (or 13.5 cm) in 50 years after impoundment. The relative settlements calculated using this method are shown in Fig. 18 for the periods before and after impoundment.

Table 5 presents a summary of estimated parameters for post-construction settlements of La Yesca dam. The second method yields smaller settlement parameters compared to the first method. The settlements of La Yesca dam during construction were small compared to similar dams. This yields very large modulus for rockfill and consequently, small values for post-construction settlement. It is expected that the values from the modulus method will yield more reliable estimations. It must be noted that as the annual rainfall histogram of the dam indicates, the impoundment period of the dam includes two rainy seasons with maximum monthly precipitation of 300 mm. Therefore, it can be anticipated that the settlements during impoundment would be higher than the estimated values due to wetting collapse, especially if the rockfill had not been sluiced during construction.

Limitations of the presented methods

In this study, the UCS of intact rock was used to characterize rock quality. However, the susceptibility of the rock to lose its strength while in contact with water, which leads to collapse due to wetting in rockfill, must also be considered. This aspect is of essential importance in areas with high precipitation and where rockfill is not watered during construction. The Roadford asphaltic concrete face rockfill (sandstone and mudstone) dam (Charles 2008) and the Martin Gonzalo concrete face rockfill (slate and greywacke) dam (Justo and Durand 2000) are two examples of impervious upstream face dams where significant wetting collapse settlement has taken place. Compared to the other cases evaluated in this study, the moduli at end of construction values are very low for Roadford and Martin Gonzalo (32 and 16 MPa, respectively). Therefore, low rockfill secant modulus at end of construction can also be an indicator of susceptibility to wetting collapse. This aspect needs further investigation.

It must also be noted that the presented method is a phenomenological approach. While all of the estimations and calculations in this study depend on the definition of the time datum, according to Leroueil (2001), any change in the time frame datum must not change results of the response of a system due to the axiom of objectivity. Nevertheless, the guidelines presented here yield a representative engineering estimation of the post-construction behavior of the CFRDs.

Conclusions

In the presented study, the post-construction crest settlement of CFRDs is linked to the in situ mechanical properties of rockfill during construction and the geometry of the embankment through an empirical method. The presented methods can be used to overcome some limitations of numerical models and laboratory experiments, such as scale effects, difference between densities and moisture contents in the field and in the laboratory, diversity of materials in a rockfill embankment, and complexity of stress paths in the field. Additionally, after assessment of the time-dependent settlements of the studied cases, aging is shown to significantly influence the settlement rates for compacted rockfill within the high strength category.

Acknowledgements

The authors gratefully acknowledge the financial support of the Natural Sciences and Engineering Research Council of Canada (NSERC) – Hydro-Québec Industrial Research Chair for life cycle optimization of embankment dams. The authors also extend their appreciation to their industrial partners: Hydro-Québec, SNC-Lavalin, Qualitas, WSP, Golder Associates, Klohn Crippen Berger, ConeTec, and Hatch.

References

Alonso, E.E., Olivella, S., and Pinyol, N.M. 2005. A review of Beliche Dam. Géotechnique, **55**(4): 267–285. doi:10.1680/geot.2005.55.4.267.

Alonso, E.E., Tapias, M., and Gili, J. 2012. Scale effects in rockfill behaviour. Géotechnique Letters, **2**(3): 155–160. doi:10.1680/geolett.12.00025.

Charles, J.A. 2008. The engineering behaviour of fill materials: the use, misuse and disuse of case histories. Géotechnique, **58**(7): 541–570. doi:10.1680/geot.2008.58.7.541.

Clements, R.P. 1981. The deformation of rockfill; inter-particle behaviour, bulk properties and behaviour in dams. King's College, London.

Clements, R.P. 1984. Post-construction deformation of rockfill dams. Journal of Geotechnical Engineering, **110**(7): 821–840. doi:10.1061/(ASCE)0733-9410(1984)110:7(821).

Colliat-Dangus, J.L., Desrues, J., and Foray, P. 1988. Triaxial testing of granular soil under elevated cell pressure. *In* Advanced triaxial testing of soil and rock. ASTM STP977. ASTM. pp. 290–310. doi:10.1520/STP29082S.

Cooke, J.B. 1984. Progress in rockfill dams. Journal of Geotechnical Engineering, **110**(10): 1381–1414. doi:10.1061/(ASCE)0733-9410(1984)110:10(1381).

Cormier, V., and Konrad, J.-M. 2015. Short and long term compressibility of rock particle assemblages. *In* Proceedings of the 68th Canadian Geotechnical Conference; GéoQuébec, Que., 20–23 September.

Fitzpatrick, M.D., Cole, B., Kinstler, F., and Knoop, B. 1985. Design of concrete-faced rockfill dams. *In* Proceedings of the Symposium on Concrete Face Rockfill Dams - Design, Construction and Performance, Detroit, Michigan. *Edited by* Cooke and Sherard. ASCE, New York. pp. 410–434.

Giudici, S., Herweynen, R., and Quinlan, P. 2000. HEC experience in concrete faced rockfill dams - past, present and future. *In* Proceedings of the International Symposium on Concrete Faced Rockfill Dams, Beijing. pp. 29–46.

Hunter, G., and Fell, R. 2002. The deformation behaviour of rockfill. The University Of New South Wales, School Of Civil And Environmental Engineering. UniCiv Report No. R-405. [January.]

ICOLD. 2010. Concrete face rockfill dams: concepts for design and construction. Bulletin 141. ICOLD.

Justo, J.L., and Durand, P. 2000. Settlement-time behaviour of granular embankments. International Journal for Numerical and Analytical Methods in Geomechanics, **24**(3): 281–303. doi:10.1002/(SICI)1096-9853(200003)24:3<281::AID-NAG66>3.0.CO;2-S.

Kermani, M. 2016. Prediction of post-construction settlements of rockfill dams, based on construction field data. Ph.D. thesis, Université Laval.

Lambe, T.W. 1973. Predictions in soil engineering. Géotechnique, **23**(2): 151–202. doi:10.1680/geot.1973.23.2.151.

Leroueil, S. 2001. Natural slopes and cuts: movement and failure mechanisms. Géotechnique, **51**(3): 197–243. doi:10.1680/geot.2001.51.3.197.

Marachi, N.D., Chan, C.K., Seed, H.B., and Duncan, J.M. 1969. Strength and deformation characteristics of rockfill materials. University of California, Berkeley. Report No. TE-69-5.

Marengo-Mogollón, H., and Rivera-Constantino, R. 2012. Geotechnical design for "La Yesca" dam: description of its behavior during the construction stage and first filling. *In* Proceedings of the CDA Annual Conference, Saskatoon, Sask., 22–27 September 2012.

Marsal, R.J. 1973. Mechanical properties of rockfill. *In* Embankment dam engineering (Casagrande Volume). *Edited by* R.C. Hirschfeld and S.J. Poulos. pp. 109–200.

Marulanda, A. 2013. Recent successful very high CFRD's. *In* Proceedings of the Annual Canadian Dam Association (CDA) Conference, Montréal, Que.

Mesri, G., and Godlewski, P.M. 1977. Time- and stress-compressibility interrelationship. Journal of the Geotechnical Engineering Division, ASCE, **103**(GT5): 417–430.

Mesri, G., and Vardhanabhuti, B. 2009. Compression of granular materials. Canadian Geotechnical Journal, **46**(4): 369–392. doi:10.1139/T08-123.

Milligan, V., and Coyne, L. 2005. Review of factors influencing the settlement of rockfill dams. *In* Proceedings of the K.Y. Lo Symposium. The University of Western Ontario. pp. 1–31.

Oldecop, L.A., and Alonso, E.E. 2007. Theoretical investigation of the time-dependent behaviour of rockfill. Géotechnique, **57**(3): 289–301. doi:10.1680/geot.2007.57.3.289.

Parkin, A.K. 1977. The compression of rockfill. Australian Geomechanics Journal, **G7**: 33–39.

Pinto, N.D., and Marques Filho, P.L. 1998. Estimating the maximum face deflection in CFRDs. International Journal on Hydropower and Dams, **5**: 28–32.

Ramon, A., Alonso, E.E., and Romero, E.E. 2008. Grain size effects on rockfill constitutive behavior. *In* Unsaturated Soils. Advances in Geo-Engineering: Proceedings of the 1st European Conference on Unsaturated Soils, Durham, UK, 2001. pp. 341–347. ISBN 978-0-415-47692-8.

Sowers, G.F., Williams, R.C., and Wallace, T.S. 1965. Compressibility of broken rock and the settlement of rockfills. *In* Proceedings of 6th ICSMFE, Montréal, Que. Vol. 2, pp. 561–565.

Soydemir, C., and Kjaernsli, B. 1979. Deformations of membrane-faced rockfill dams. *In* Proceedings of the 7th European Conference on Soil Mechanics and Foundation Engineering, Brighton, England. pp. 281–284.